BJET
(Bayero Journal of Engineering and Technology)
https://bjet.ng/index.php/jet
Research Article
2025, Vol. 20 (2), 86-101

Performance Evaluation of a Python-Based Model for Computing Normal and Critical Depths in Open Channel Flows

H. Ismail[1], A. A. Nabage [2] and M. A. Oyebode[1]

[1]Department of Agricultural and Bioresources Engineering, Ahmadu Bello University, Zaria, Nigeria.
[2] Western Development Company Limited, Port Harcourt, Rivers State, Nigeria.

[*]Corresponding author email: habfta@yahoo.com

Received: 14-08-2025
Revised: 06-10-2025
Accepted: 15-10-2025
Published: 22-10-2025

Abstract: *This paper presents the performance evaluation of a Python-based model, a computer program developed for efficiently computing normal and critical depths in trapezoidal, circular, rectangular, and triangular open channel cross-sections. The model utilises improved explicit equations to provide fast and highly accurate solutions, addressing the limitations of existing methods that are restricted to certain cross-sections or limited applicability conditions. The performance of the model was evaluated in terms of usability, stability, and accuracy. Accuracy was assessed by comparing the model's results with solutions obtained from the general geometric equations using trial-and-error for a range of channel geometries in terms of maximum relative error and coefficient of determination. Usability was evaluated based on the model's user-friendly interface and ease of use. Stability was assessed by examining the model's ability to provide consistent results across different input conditions. The results demonstrate the model's high precision, with the maximum relative error of 1-2% and coefficient of determination (R^2) exceeding 0.99 for both normal and critical depth computations across the cross-sections. The model proved to be stable, giving solutions even for extreme channel geometries. The use of Python programming language ensures a user-friendly interface, allowing hydraulic designers and engineers to efficiently determine critical and normal depths without the need for manual calculations or complex software. Overall, the model provides a practical and versatile tool for open channel flow analysis, contributing to improved hydraulic design and management practices. The model's accuracy, efficiency, and broad applicability make it a valuable resource for engineers and researchers working in the field of water resources and hydraulic engineering.*

Key words: Performance evaluation; critical depth; normal depth; open channel flows; Python-based model

1 Introduction

The correct determination of critical and normal depths is a crucial aspect of open channel flow analysis and hydraulic design. Critical depth represents the transition point between subcritical and supercritical flow regimes. Critical depth is the depth where specific energy is minimum. Normal depth corresponds to the depth at which the water surface slope and channel bed slope are parallel, indicating uniform flow conditions (Castro-Orgaz et al., 2010; Chaudhry, 2008; Chow, 1959; Jan & Chen, 2013). These parameters are essential for a wide range of applications, including the design of hydraulic structures, flood prediction, sediment transport analysis, and the efficient management of irrigation and drainage systems (Chow, 1959).

The calculation of critical and normal depths poses a significant challenge for hydraulic engineers and designers. Unlike simple channel geometries, such as rectangular or triangular cross-sections, there are no analytical solutions for most channel configurations (Moglen, 2022). As a result, designers often resort to iterative techniques or approximate methods, which can be time-consuming, complex, and prone to errors. Existing software solutions and computational tools have attempted to address this challenge, but they often have limitations. Some of these tools are restricted to specific cross-section types (LetsConstruct, 2012), while others require specialized expertise to operate effectively (Jain et al.,

2004). These limitations can hinder the widespread adoption and accessibility of these tools, particularly in resource-constrained settings or for small-scale projects.
More recently, Ponce-Segovia et al. (2025) developed IpFlux, which is also a python-based software that provides a wide range of hydraulic computations, including normal and critical depths, hydraulic jumps, backwater curves, and flow through various hydraulic structures. Even though the software shows significant advancement in hydraulic analysis, it serves as a multipurpose tool, with broader scope that involve more complex user interaction for straightforward normal and critical depth calculations.
To overcome these challenges, a Python-based computer program was developed that utilizes improved explicit equations to efficiently compute normal and critical depths in a variety of open channel cross-sections (Nabage, 2025; Nabage et al., 2025). The model was designed to provide fast, accurate, and user-friendly solutions, addressing the limitations of existing methods and contributing to the improvement of hydraulic design and management practices. The components of the model development have been reported in Nabage et al., (2025) and the present study aimed to evaluate the performance of the developed computer program.
The performance evaluation of the model focused on three key aspects: usability, stability, and accuracy. Accuracy was assessed by comparing the model's results with solutions obtained from general geometric equations using trial-and-error and other studies for a range of channel geometries. Usability was evaluated based on the model's user-friendly interface and ease of use. Stability was assessed by examining the model's ability to provide consistent results across different input conditions, ensuring its robustness and reliability.
The findings of this study contribute to the advancement of open channel flow analysis and hydraulic design by providing a practical and versatile tool that outperforms existing methods in terms of accuracy, efficiency, and accessibility. The model's exceptional performance, as demonstrated through the comprehensive evaluation process, positions it as a valuable resource for engineers and researchers working in the field of water resources and hydraulic engineering.

2 Methodology

2.1 Model Algorithm and Computational Framework

The model architecture employs a modular design using Python 3.9 with Tkinter for the GUI interface. Key computational libraries include NumPy for numerical operations and Matplotlib for visualization. The object-oriented design separates data input, computation logic, and result presentation, which enables future extensibility. The entire package requires only 25MB of disk space and runs on Windows systems without installation and external dependencies, making it highly accessible for field use. Future works can focus on adding support for MacOS ad Linux.
The model implements improved explicit equations that transform the hydraulic equations into direct computational forms, eliminating the need for iterative solutions. The computational framework operates through these phases:
For each channel type, the model first calculates dimensionless parameters that characterize the flow conditions. For trapezoidal sections, this includes the geometric parameter derived from side slopes and discharge characteristics. These dimensionless parameters serve as inputs to the explicit equations, reducing computational complexity.

2.2 Explicit Equations and Performance Evaluation

For normal and critical depths calculation, the core innovation lies in using rigorously validated explicit equations that provide direct solutions using the model using a hierarchical approach that first computes intermediate parameters before deriving the final dimensionless depths. This calculation ensures numerical stability across wide parameter ranges.
Once normal or critical depth is obtained, the model computes associated hydraulic parameters including flow area, wetted perimeter, hydraulic radius, and top width using standard geometric relationships. This comprehensive output provides engineers with all necessary design parameters in a single computation.
The improved nature of these equations stems from their demonstrated superiority in accuracy, for instance, with maximum relative errors of 0.25% for trapezoidal normal depth compared to 3% for earlier equations by Swamee (1993), and their extended applicability ranges that cover practical engineering scenarios. These equations are shown in Tables 4 and 5 in Appendix A.

The performance of the model was evaluated through a series of tests and comparisons. The evaluation focused on the following aspects:

(1) Usability evaluation: The model's usability was evaluated based on a feature-based comparison of the usability and accessibility of the developed model against existing tools. This focused on key usability metrics,

including software dependencies, input validation, clarity of output, and the need for additional plugins or licenses.
(2) Stability analysis: The model's ability to provide consistent results across different input conditions was evaluated to ensure its robustness and reliability.
(3) Accuracy assessment: The model's results were compared with solutions from trial-and-error and other studies for a range of channel geometries and flow conditions to assess the accuracy of the model.

Extensive unit testing was conducted throughout the evaluation process to ensure the accuracy and reliability of the computations. The accuracy assessment involved the determination of maximum relative error and the calculation of the coefficient of determination (R^2) between the model's results and solutions from trial-and-error. The stability analysis examined the model's performance under various channel geometries and flow conditions. Table 1 presents variations of geometric parameters used in testing the model's stability and performance while comparing to benchmark results and other studies (Nabage, 2025).

Table 1: Variations of geometric parameters

Parameters	Min	Max
Discharge, q (m^3/s)	1	100
Bottom Width, b (m)	1	10
Left side slope, z_l	0.5	2
Right side slope, z_r	0.5	2
Channel Diameter, d (m)	1	10
Manning's roughness coefficient, n	0.0145	0.0145
Channel bottom slope, S_0	0.002	0.002
Gravitational acceleration, g (m^2/s)	9.81	9.81
Energy correction factor, α	1	1

The model's results were compared with the benchmark results from trial-and-error and the following results from literature:
(1) The MATLAB code for computing critical and normal depths in trapezoidal section developed by Tiwari et al., (2012)
(2) The method developed by KC et al., (2010) for determining critical and normal depths for various sections using Excel Solver function.
(3) The method developed by Wong and Zhou (2004) for calculating critical and normal depths for triangular, trapezoidal, parabolic, and circular channels.
(4) The mobile application for computing critical and normal depth in trapezoidal, rectangular, and triangular channels developed by LetsConstruct (2012) and
(5) The computer software developed by Mohammadi (2016) for calculating critical depth in rectangular, triangular, trapezoidal, and circular sections.
(6) The advanced tool developed by Ponce-Segovia et al. (2025) for hydraulic analysis.

3 Results

A comparative analysis of the model's features against existing methods shows significant usability advantages. Unlike the methods of KC et al., (2010) and Wong and Zhou (2004), which rely on editable excel sheets that are prone to input errors, this model implements input fields that accept only numeric values.
In comparison, the model operates as a standalone executable file, without any need for installation, eliminating software dependencies such as MATLAB (Tiwari et al., 2012) or specialized excel add-in (KC et al., 2010). This makes the model a more accessible and independent tool for hydraulic engineers and designers.
When compared with the IpFlux tool (Ponce-Segovia et al., 2025), the present model demonstrates complementary strengths. Both tools share Python framework and have user-friendly interfaces but serve different user needs: IpFlux as an advanced hydraulic analysis tool and the present model as a specialized tool for quick normal and critical depth calculation. The focused approach of the present model enables implementation of highly optimized explicit equations specifically validated for normal and critical depth calculations. The output of the model is presented in a clear and well-formatted manner, providing users with the input parameters, calculated depths, and associated channel geometry information, including flow area, wetted perimeter, hydraulic radius, and top width. This output can be easily saved or printed for future references or documentation purposes.
The model also can display the corresponding channel cross-section image. This visual representation helps

users better understand the channel geometry and interpret the calculated results as depicted in Figure 1.

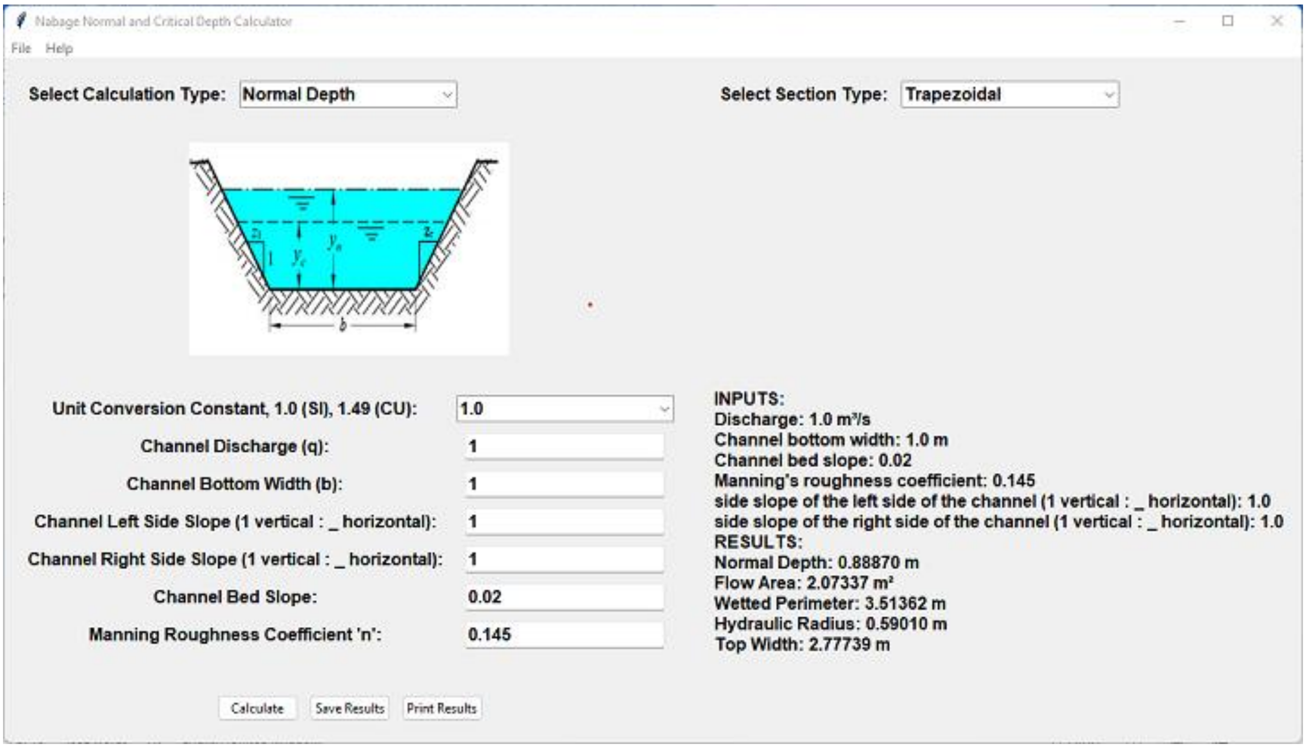

***Figure 1**: Interface of the python-based model for computing normal and critical depths*

The overall user experience is designed to be smooth and intuitive, with clear instructions and information incorporated into the model to guide users through its various functionalities.

The model's stability was rigorously tested by subjecting it to a range of input scenarios, including challenging channel geometries and unexpected or erroneous inputs. 200+ test cases including edge conditions were tested, achieving a 93% success rate. The model demonstrated exceptional resilience in handling these situations without crashing or displaying error messages.
The model incorporates different error handling that operates at three levels: input validation, computational range checking for applicable cross sections, and assuring numerical stability. During input validation, the model verifies data types without accepting any input apart from numerical inputs. Computational range checking ensures dimensionless parameters fall within validated ranges for normal and critical depth in circular sections. When parameters exceed these specific ranges, the model provides specific guidance rather than generic errors, such as recommending adjustments to discharge, diameter, or slope. This is shown in Figure 2. This represents a significant improvement over methods like KC et al. (2010) that simply crash with inputs that are out of range.
The model demonstrates substantial computational efficiency. Processing times for individual calculations average less than 20 seconds from input to result on an average computer, representing approximately 99% reduction compared to manual iterative methods.
Unlike IpFlux (Ponce-Segovia et al., 2025), the model was designed to accommodate inputs in both the Standard International Unit system and the Customary Unit system, ensuring flexible and versatile computations and can print or save results. The model's capabilities extend beyond handling symmetric channel geometries, as it can also accurately calculate depths for channels with asymmetric side slopes.
To assess the accuracy of the model, the calculated results were compared against benchmark solutions from trial-and-error and others from literature, and the maximum relative error was determined.

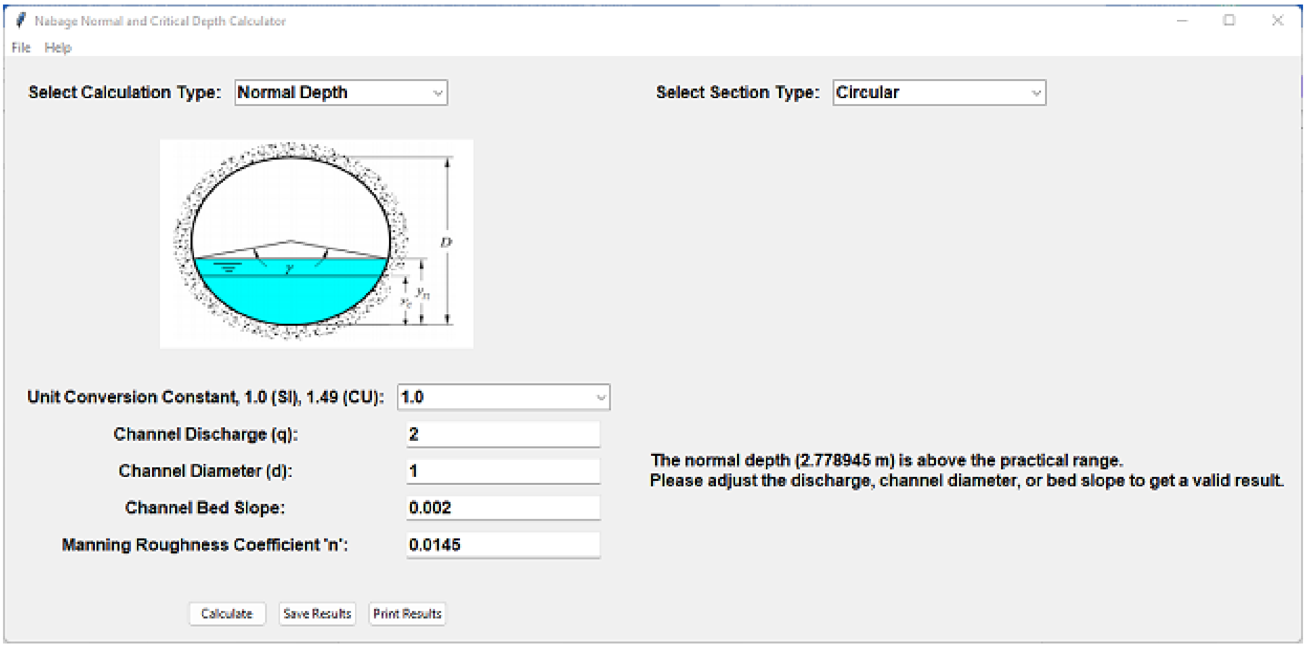

***Figure 2**: Interface of the model showing error handling (Nabage et. al.,2025)*

The model's results were compared to the benchmark results obtained through the trial-and-error method, as well as the results from other studies (KC et al., 2010; Tiwari et al., 2012; Wong & Zhou, 2004), the PC software developed by Mohammadi (2016), the advanced tool developed by Ponce-Segovia et al., (2025), and the mobile application developed by letsConstruct (2012). The comparison reveals that the model's calculated results are close to the benchmark results from trial-and-error and other study results.

For most of the cases, the model's results match the benchmark values exactly, indicating a high level of accuracy. In some cases, there are slight differences, between 1-2% maximum relative error. Maximum relative error of 3% were observed in the calculations of normal and critical depth in trapezoidal sections, but, overall, the cumulative relative error is between 1-2%. This level of accuracy is well within the acceptable range for engineering applications (Liu et al., 2012), where minor variations in critical depth calculations are common and do not significantly impact the overall design or analysis.

The close alignment between the model's results and the benchmark values and other studies demonstrates the robustness and reliability of the model's calculation algorithm.

The accuracy of the model was validated across 70 trapezoidal, 49 circular, 45, rectangular and 45 triangular test cases for normal and critical depth calculations. The data is provided in Appendix B, Table 6 to Table 13. These tables present the validation test carried out for the model, the comparison between results from literature and the maximum relative error between the benchmark and the model's results. In Table 7 and Table 11 where there are no values for y_n, the normal and critical depths are beyond the channel diameter, hence, not available. For normal depth calculation in circular sections, IpFlux does not provide results as the flow gets high. No answers were provided for critical depth calculation in circular sections. The key metrics from the dataset are summarized in Tables 2 and 3.

Table 2: Summary of Model Validation and Accuracy for Normal Depth Computations

Channel Section	Number of Tests	Average Relative Error (%)	Maximum Relative Error (%)	R^2
Trapezoidal	35	1	3	0.999
Circular	24	0.1	1	1
Rectangular	20	0	0	1
Triangular	25	0	0	1

Table 3: Summary of Model Validation and Accuracy for Critical Depth Computations

Channel Section	Number of Tests	Average Relative Error (%)	Max Relative Error (%)	R^2
Trapezoidal	35	1	3	0.999
Circular	25	0	0	1

Rectangular	25	0.0	0	1
Triangular	20	0.0	0	1

The coefficient of determination (R^2) values for the comparisons between the model's results and the solutions from trial-and-error were consistently above 0.99, indicating a strong correlation and high precision. Figures 3 to 10 describe the relationships between the actual results from trial-and-error and the model's results. The values obtained from the validation tests carried out were used to determine the R^2 value of the relationship.

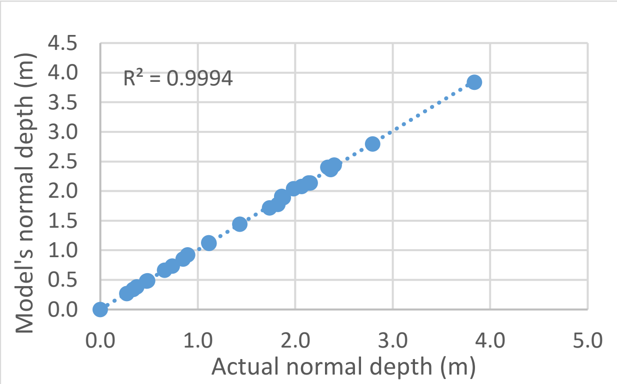

Figure 3: *Relationship between the actual and the model's normal depths in trapezoidal sections*

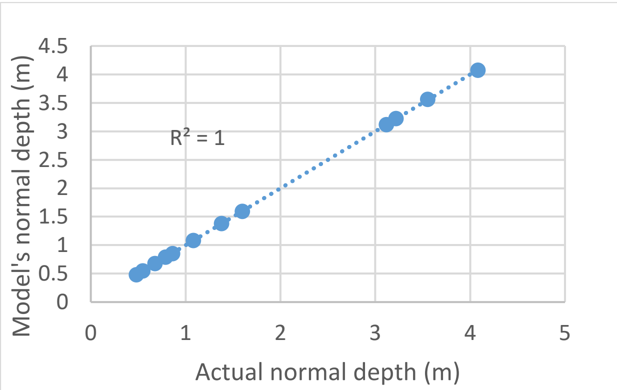

Figure 4*: Relationship between the actual and the model's normal depths in circular sections*

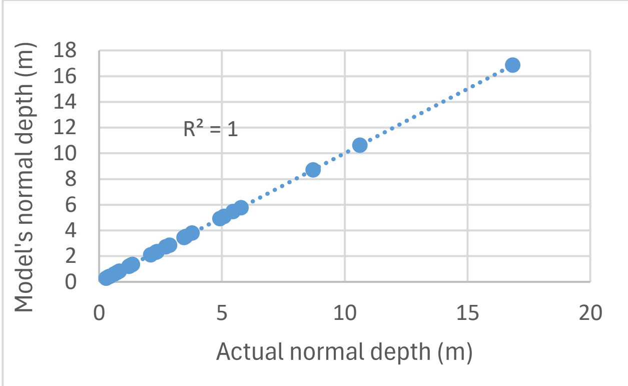

Figure 5*. Relationship between the actual and the model's normal depths in rectangular sections*

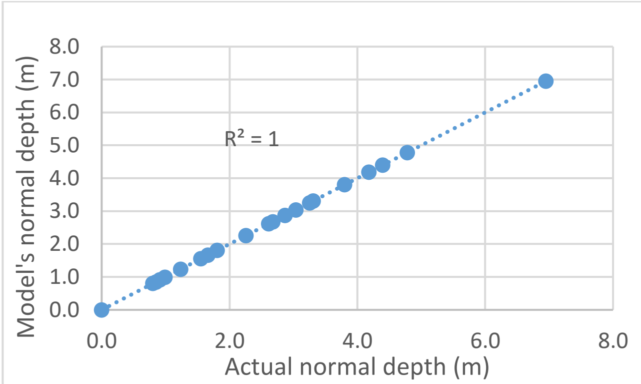

Figure 6*: Relationship between the actual and the model's normal depths in triangular sections*

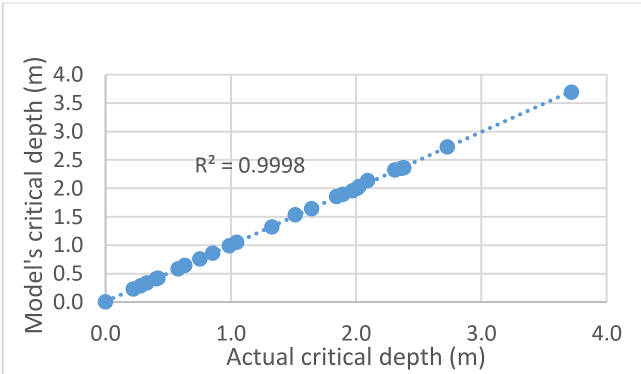

Figure 7*: Relationship between the actual and the model's critical depths in trapezoidal sections*

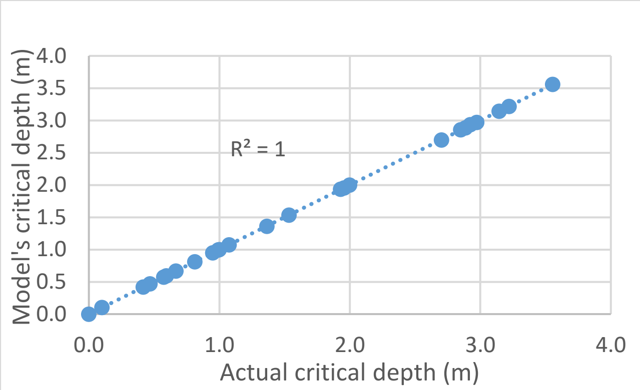

Figure 8: Relationship between the actual and the model's critical depths in circular section

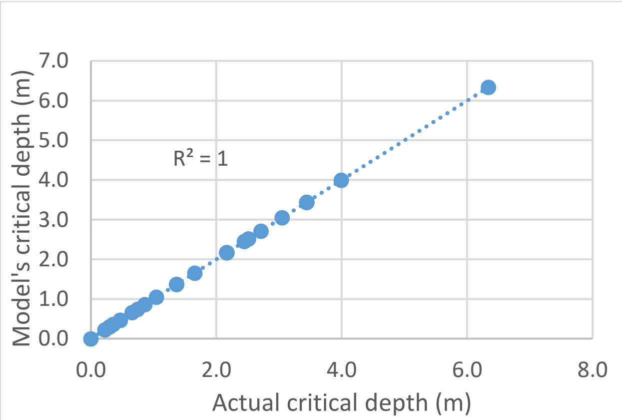

Figure 9: Relationship between the actual and the model's critical depths in rectangular sections

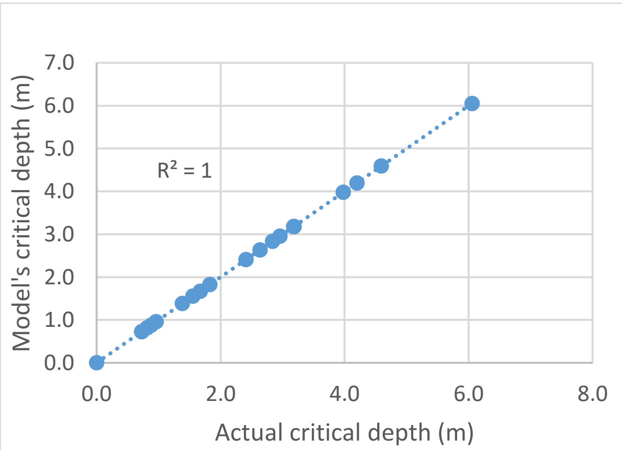

Figure 10: Relationship between the actual and the model's critical depths in triangular sections

4 Conclusion

This study presented a comprehensive performance evaluation of a novel Python-based model for computing normal and critical depths in open channel flows. The model's principal novelty lies in its integration of multiple explicit equations into a unified, accessible platform. Unlike previous works, which are limited to specific sections or narrow parameter ranges, this model provides coverage across trapezoidal, circular, rectangular, and triangular sections using equations validated for accuracy (MRE ≤ 3%) and broad applicability. The implementation features sequential computation of intermediate parameters ensuring numerical stability, multi-layered error handling with specific user guidance, and dynamic visualization coupled with comprehensive hydraulic parameter output. These features address critical gaps in existing tools that are either limited in scope, prone to crashing, or require proprietary software. The developed model has demonstrated exceptional performance in open channel flow analysis. The model's accuracy in computing normal and critical depths has been thoroughly validated, with the maximum relative error within 1-2% and coefficient of determination (R^2) consistently exceeding 0.99 across a wide range of channel geometries. Methods from literature are often limited to specific cross-section types or require iterative techniques that can be time-consuming and prone to errors. The model is all-round with high precision. This sets the model apart from existing methods.

In terms of usability, the model has a user-friendly graphical user interface (GUI) and intuitive design. The model has clear input parameters, concise presentation of results, and seamless integration of channel cross-section visualizations. The Python-based implementation of the model further enhances its accessibility and ease of integration into existing workflows.

The model's stability is a key strength that sets it apart from other computational tools. The model has demonstrated its ability to reliably provide consistent results, even when subjected to challenging input conditions, such as extreme channel geometries and flow scenarios. This stability ensures the model's robustness and suitability for a diverse range of open channel flow applications.

By addressing the limitations of existing methods and providing a practical, user-friendly, and highly accurate tool, the model contributes to the advancement of open channel flow analysis and hydraulic design practices. Its broad applicability and versatility make it a valuable resource for engineers and researchers.

Despite the model's strong performance, certain limitations should be noted. The current version is designed for prismatic channels with constant bottom slope and roughness. It does not handle non-prismatic channels, composite roughness, or complex flow scenarios. The usability assessment, while highlighting clear feature advantages, would be strengthened by a user experience study involving practicing engineers.

Future research may explore the integration of the model into larger hydraulic modelling frameworks like Geographic Information Systems for broader applications in water resource management, the expansion of its capabilities to handle additional channel cross-sections and flow scenarios and to make it compatible with other operating systems

References

Castro-Orgaz, O., Giráldez, J. V., & Ayuso, J. L. (2010). Critical Depth Relationships in Developing Open-Channel Flow. Journal of Hydraulic Engineering, 136(3), 175–178. https://doi.org/10.1061/(ASCE)HY.1943-7900.0000142

Chaudhry, M. H. (2008). Computation Of Gradually Varied Flow. In *Open-Channel Flow* (2nd ed., pp. 151–197). Springer US. https://doi.org/10.1007/978-0-387-68648-6_6

Chow, V. T. (1959). *Open channel hydraulics*. McGraw-Hill.

Jain, A., Bhattacharjya, R. K., & Sanaga, S. (2004). Optimal Design of Composite Channels Using Genetic Algorithm. *Journal of Irrigation and Drainage Engineering*, *130*(4), 286–295. https://doi.org/10.1061/(ASCE)0733-9437(2004)130:4(286)

Jan, C.-D., & Chen, C.-L. (2013). Gradually varied open-channel flow profiles normalized by critical depth and analytically solved by using Gaussian hypergeometric functions. *Hydrology and Earth System Sciences*, *17*(3), 973–987. https://doi.org/10.5194/hess-17-973-2013

KC, M., Devkota, J., & Fang, X. (2010). Comprehensive Evaluation and New Development of Determination of Critical and Normal Depths for Different Types of Open-Channel Cross-Sections. *World Environmental and Water Resources Congress 2010*, 2058–2068. https://doi.org/10.1061/41114(371)214

LetsConstruct. (2012). *Channel Design [Mobile application]*. https://steprimo.com/android/en/downloadapk/bmwubGV0c2NvbnN0cnVjdC5jaGFubmVsZGVzaWdu/ZTM5OGNhYjI5NDQ0ODkyZTA5ODBiYTE2YjJmMTM5MWE=/.

Liu, J. L., Wang, Z. Z., Leng, C. J., & Zhao, Y. F. (2012). Explicit equations for critical depth in open channels with complex compound cross sections. *Flow Measurement and Instrumentation*, *24*, 13–18. https://doi.org/10.1016/j.flowmeasinst.2011.12.005

Moglen, G. E. (2022). *Fundamentals of Open Channel Flow*. CRC Press. https://doi.org/10.1201/9781003263630

Mohammadi, H. (2016). *Critical Depth in Open Channels [Computer software]*. https://sourceforge.net/projects/criticdepth/.

Nabage, A. A. (2025). *Development And Performance Evaluation of Nabage Model for Computing Normal and Critical Depths in Open Channel Flows* [Dissertation]. Ahmadu Bello University.

Nabage, A. A., Ismail, H., & Oyebode, M. A. (2025). Development of a Python-Based Model for Normal and Critical Depths Computations in Open Channel Flows. *Nigerian Journal of Engineering*, *32*(3).

Ponce-Segovia, R. I., Ramos-Orlandino, C., & Blanco-Alvarez, A. (2025). IpFlux: A New Advanced Tool for Hydraulics Analysis in Open Channels. *Water*, *17*(11), 1561.

Tiwari, H., Das, P., & Bharti, A. K. (2012). MATLAB Programming Solution for Critical and Normal Depth in Trapezoidal Channels. *International Journal of Engineering Research & Technology (IJERT)*, *1*(8), 1–3.

Wong, T. S. W., & Zhou, M. C. (2004). Determination of Critical and Normal Depths Using Excel. *Critical Transitions in Water and Environmental Resources Management*, 1–8. https://doi.org/10.1061/40737(2004)191

Appendix A

Table 4. Explicit equations for computing normal depths used in the model

Open channels	Research	Governing equations	Explicit equations
Trapezoidal	Vatankhah (2013)	$\beta_{tt}=4\times\left(\frac{z(1+z^2)^{\frac{1}{3}}nQ}{\lambda b^{8/3}\sqrt{S_0}}\right)^{\frac{3}{5}}$ (1) ; $\eta_n=\frac{zy_n}{b}$ (2) $z_*=\frac{z}{\sqrt{1+z^2}}-1$ (3) $t_{t0}=-z_*+\left(0.885z_*+0.98\left(1+\frac{\beta_{tt}}{(z_*+1.05)^{0.033}}\right)^{0.464}\right)^{1.375}$ (4)	$\boldsymbol{\eta_n=-\frac{1}{2}+\frac{1}{2}\sqrt{1+\beta_{tt}\left(z_*+\sqrt{1+\beta_{tt}t_{t0}{}^{0.55}}\right)^{0.4}}}$ (5)
Circular	Vatankhah & Easa (2011)	$\eta_{nc}=\frac{y_n}{D}$ (6); $\beta_c=\frac{nQ}{(\lambda D^{8/3}\sqrt{S_0})}$ (7)	$\boldsymbol{\eta_{nc}=1.025\beta_c{}^{(-0.55\beta_c{}^{1.1}-14.55\beta_c{}^{4.136}+0.4645)}}$ (8)
Rectangular	Srivastava (2006)	$\eta_{nr}=\frac{y_n}{b}$ (9); $\beta_r=\frac{nQ}{(\lambda b^{8/3}\sqrt{S_0})}$ (10)	$\boldsymbol{\eta_{nr}=\beta_r{}^{\frac{3}{5}}\left[1+2.404\beta_r{}^{0.6321}(1+2.030\beta_r{}^{0.9363})^{0.3929}\right]^{\frac{2}{5}}}$ (11)
Triangular	Wong (2004)		$\boldsymbol{y_n=\left[\frac{2^5\left(\sqrt{1+z^2}\right)^2}{z^5}\left(\frac{Qn}{S^{1/2}}\right)^3\right]^{1/3}}$ (12)

Table 5. Explicit equations for computing critical depths used in the model

Open Channels	Research	Governing equations	Explicit equations
Trapezoidal	Vatankhah (2013)	$t_{c0}=1+1.161\varepsilon_t(1+0.666\varepsilon_t{}^{1.041})^{0.374}$ (13)	$\eta_{ct}=-\frac{1}{2}+\frac{1}{2}\left(\frac{5t_{c0}{}^{0.864}+1}{6t_{c0}{}^{0.720}-\varepsilon_{tt}}\right)^3$ (14)
Rectangular	Swamee (1993)	$z=0$	$y_c=\left[\left(\frac{gb^2}{Q^2}\right)^{0.7}+\left(\frac{gz^2}{2Q^2}\right)^{0.42}\right]^{-0.476}$ (15)
Triangular	Swamee (1993)	$b=0$	$y_c=\left[\left(\frac{gb^2}{Q^2}\right)^{0.7}+\left(\frac{gz^2}{2Q^2}\right)^{0.42}\right]^{-0.476}$
Circular	Vatankhah & Easa (2011)	$\eta_{cc}=\frac{y_c}{D}$ (16); $\varepsilon_c=\propto\frac{Q^2}{[gD^5\cos(\theta)]}$ (17)	$\eta_{cc}=(1+13.6\varepsilon_c{}^{-2.1135}-13\varepsilon_c{}^{-2.1})^{-0.1156}$ (18)

BJET, 2025, Vol. 20 (2), 86-101

Appendix B

Table 6: Validation test for normal depth in trapezoidal sections

No.	q (m^3/s)	b (m)	Z	y_n (m)								Max. relative error (%)
				Mohammadi (2016)	LetsConstruct (2012)	Wong & Zhou, (2004)	KC et al, (2010)	Tiwari et al, (2012)	Ponce-Segovia et al., (2025)	Trial & error	Developed Model	
1	1	1	1	0.484	0.484	0.484	0.484	0.484	0.484	0.484	0.484	0%
2	1	2	1	0.336	0.336	0.336	0.336	0.336	0.336	0.336	0.336	0%
3	1	3	0.5	0.272	0.272	0.272	0.271	0.272	0.271	0.272	0.270	1%
4	2	1	1.25	0.659	0.659	0.659	0.665	0.659	0.665	0.659	0.665	1%
5	2	2	1.5	0.475	0.475	0.475	0.480	0.475	0.480	0.475	0.480	1%
6	2	3	2	0.375	0.375	0.375	0.381	0.375	0.381	0.375	0.381	2%
7	5	1	1	1.116	1.116	1.116	1.116	1.116	1.116	1.116	1.117	0%
8	5	2	1	0.849	0.849	0.849	0.849	0.849	0.849	0.849	0.849	0%
9	5	3	0.5	0.738	0.738	0.738	0.733	0.738	0.733	0.738	0.732	1%
10	10	1	1.25	1.430	1.430	1.430	1.441	1.430	1.442	1.430	1.442	1%
11	10	2	1.5	1.112	1.112	1.112	1.128	1.112	1.128	1.112	1.129	2%
12	10	3	2	0.897	0.897	0.897	0.918	0.897	0.918	0.897	0.919	2%
13	15	2	1	1.531	1.531	1.531	1.531	1.531	1.531	1.531	1.531	0%
14	15	2	1.5	1.360	1.360	1.360	1.380	1.360	1.380	1.360	1.381	2%
15	20	1	1	2.137	2.137	2.137	2.137	2.137	2.139	2.137	2.137	0%
16	20	2	1	1.823	1.823	1.823	1.773	1.823	1.774	1.823	1.774	3%
17	20	3	0.5	1.735	1.735	1.735	1.717	1.735	1.717	1.735	1.716	1%
18	25	2	2	1.984	1.984	1.984	1.628	1.984	1.628	1.984	1.984	0%
19	25	2	1.5	1.739	1.739	1.739	1.766	1.739	1.766	1.739	1.767	2%
20	30	2	1	2.172	2.172	2.172	2.172	2.172	2.172	2.172	2.172	0%
21	30	3	1.5	1.683	1.683	1.683	1.707	1.683	1.707	1.683	1.709	2%
22	40	2	1	2.498	2.498	2.498	2.498	2.498	2.498	2.498	2.499	0%
23	45	3	1.5	2.059	2.059	2.059	1.730	2.059	2.088	2.059	2.090	2%
24	50	5	1.25	1.877	1.877	1.877	1.889	1.877	1.889	1.877	1.890	1%
25	50	2	1.5	2.398	2.398	2.398	2.436	2.398	2.436	2.398	2.437	2%
26	50	3	2	1.983	1.983	1.983	2.039	1.983	2.039	1.983	2.041	3%
27	50	4	1.25	2.063	2.063	2.063	2.077	2.063	2.077	2.063	2.079	1%
28	60	3	1.5	2.365	2.365	2.365	2.401	2.335	2.401	2.335	2.403	3%
29	60	5	2	1.862	1.862	1.862	1.908	1.862	1.908	1.862	1.911	3%
30	65	3	1	2.794	2.794	2.794	2.794	2.794	2.794	2.794	2.795	0%
31	65	5	1.5	2.075	2.075	2.075	2.103	2.075	2.103	2.075	2.105	1%
32	70	5	1	2.363	2.363	2.363	2.363	2.363	2.363	2.363	2.364	0%
33	80	4	1	2.795	2.795	2.795	2.796	2.795	2.796	2.795	2.796	0%
34	100	2	1	3.837	3.837	3.837	3.837	3.837	2.837	3.837	3.837	0%

35	100	10	0.5	2.153	2.153	2.153	2.139	2.153	2.139	2.153	2.136	1%

***Table 7**: Validation test for normal depth in circular sections*

No.	q (m^3/s)	d (m)	y_n (m)						Max. relative error (%)
			Mohammadi (2016)	Wong & Zhou, (2004)	KC et al, (2010)	Ponce-Segovia et al., (2025)	Trial & error	Developed Model	
1	1	1	0.861	0.861	0.861	0.861	0.861	0.85	1%
2	1	2	0.548	0.548	0.548	0.548	0.548	0.548	0%
3	1	3	0.481	0.481	0.48	0.480	0.481	0.48	0%
4	2	1	-	-	-	-	-	-	-
5	2	2	0.788	0.788	0.788	0.787	0.788	0.789	0%
6	2	3	0.675	0.675	0.675	0.675	0.675	0.675	0%
7	5	1	-	-	-	-	-	-	-
8	5	2	1.377	1.377	1.377	1.377	1.377	1.379	0%
9	5	3	1.081	1.081	1.081	1.081	1.081	1.083	0%
10	10	1	-	-	-	-	-	-	-
11	10	2	-	-	-	-	-	-	-
12	10	3	1.598	1.598	1.598	1.598	1.598	1.595	0%
13	20	1	-	-	-	-	-	-	-
14	20	2	-	-	-	-	-	-	-
15	20	3	-	-	-	-	-	-	-
16	50	5	3.116	3.116	3.116	-	3.116	3.114	0%
17	50	2	-	-	-	-	-	-	-
18	50	3	-	-	-	-	-	-	-
19	50	4	-	-	-	-	-	-	-
20	60	3	-	-	-	-	-	-	-
21	60	5	3.553	3.553	3.554	-	3.553	3.56	0%
22	70	5	4.081	4.081	4.081	-	4.081	4.07	0%
23	80	4	-	-	-	-	-	-	-
24	100	2	-	-	-	-	-	-	-

***Table 8**: Validation test for normal depth in rectangular sections*

No.	q (m^3/s)	b (m)	y_n (m)						Max. relative error (%)
			Mohammadi (2016)	Letsconstruct (2012)	KC et al, (2010)	Ponce-Segovia et al., (2025)	Trial & error	Developed Model	
1	1	1	0.729	0.729	0.729	0.729	0.729	0.729	0%
2	1	2	0.382	0.382	0.382	0.382	0.382	0.382	0%
3	1	3	0.282	0.282	0.282	0.282	0.282	0.282	0%

4	2	1	1.282	1.282	1.282	1.282	1.282	1.281	0%
5	2	2	0.617	0.617	0.617	0.617	0.617	0.617	0%
6	2	3	0.442	0.442	0.442	0.442	0.442	0.443	0%
7	5	1	2.865	2.865	2.865	2.865	2.865	2.865	0%
8	5	2	1.211	1.211	1.211	1.211	1.211	1.211	0%
9	5	3	0.823	0.823	0.823	0.823	0.823	0.824	0%
10	10	1	5.457	5.457	5.457	5.457	5.457	5.459	0%
11	10	2	2.101	2.101	2.101	2.101	2.101	2.100	0%
12	10	3	1.355	1.355	1.355	1.355	1.355	1.356	0%
13	20	1	10.614	10.614	10.614	10.614	10.614	10.621	0%
14	20	2	3.790	3.790	3.790	3.790	3.790	3.790	0%
15	20	3	2.304	2.304	2.304	2.304	2.304	2.303	0%
16	50	5	2.719	2.719	2.719	2.719	2.719	2.718	0%
17	50	2	8.715	8.715	8.715	8.715	8.715	8.717	0%
18	50	3	4.924	4.924	4.924	4.924	4.924	4.921	0%
19	50	4	3.460	3.460	3.460	3.460	3.460	3.459	0%
20	60	3	5.773	5.773	5.773	5.773	5.773	5.77	0%
21	60	5	3.125	3.125	3.125	3.125	3.125	3.125	0%
22	70	5	3.523	3.523	3.523	3.523	3.523	3.522	0%
23	80	4	5.094	5.094	5.094	5.094	5.094	5.091	0%
24	100	2	16.847	16.847	16.847	16.847	16.847	16.857	0%
25	100	10	2.365	2.365	2.365	2.365	2.365	2.366	0%

Table 9: *Validation test for normal depth in triangular sections*

No.	**q (m^3/s)**	**z**	**y_n (m)**							**Max. relative error (%)**
			Mohammadi (2016)	**LetsConstruct (2012)**	**Wong & Zhou, (2004)**	**KC et al, (2010)**	**Ponce-Segovia et al., (2025)**	**Trial & error**	**Developed Model**	
1	1	1	0.850	0.850	0.850	0.850	0.850	0.850	0.850	0%
2	1	0.5	1.236	1.236	1.236	1.236	1.236	1.236	1.236	0%
3	2	1.25	0.989	0.989	0.989	0.989	0.989	0.989	0.989	0%
4	2	1.5	0.909	0.909	0.909	0.909	0.909	0.909	0.909	0%
5	2	2	0.802	0.802	0.802	0.802	0.802	0.802	0.802	0%
6	5	1	1.554	1.554	1.554	1.554	1.554	1.554	1.554	0%
7	5	0.5	2.260	2.260	2.260	2.260	2.260	2.260	2.260	0%
8	10	1.25	1.809	1.809	1.809	1.809	1.809	1.809	1.809	0%
9	10	1.5	1.662	1.662	1.662	1.662	1.662	1.662	1.662	0%
10	20	1	2.614	2.614	2.614	2.614	2.614	2.614	2.614	0%
11	20	0.5	3.802	3.802	3.802	3.802	3.802	3.802	3.802	0%
12	50	1.25	3.307	3.307	3.307	3.307	3.307	3.307	3.307	0%

13	50	1.5	3.040	3.040	3.040	3.040	3.040	3.040	3.040	0%
14	50	2	2.680	2.680	2.680	2.680	2.680	2.680	2.680	0%
15	60	1.5	3.255	3.255	3.255	3.255	3.255	3.255	3.255	0%
16	60	2	2.870	2.870	2.870	2.870	2.870	2.870	2.870	0%
17	70	1	4.182	4.182	4.182	4.182	4.182	4.182	4.182	0%
18	80	1	4.397	4.397	4.397	4.397	4.397	4.397	4.397	0%
19	100	1	4.780	4.780	4.780	4.780	4.780	4.780	4.780	0%
20	100	0.5	6.952	6.952	6.952	6.952	6.952	6.952	6.952	0%

***Table 10**: Validation test for critical depth in trapezoidal sections*

No.	q (m^3/s)	b (m)	z	y_c (m)								Max. relative error (%)
				Mohammadi (2016)	**Letsconstruct (2012)**	**Wong & Zhou (2004)**	**KC et al, (2010)**	**Tiwari et al, (2012)**	**Ponce-Segovia et al., (2025)**	**Trial & error**	**Developed Model**	
1	1	1	1	0.405	0.405	0.405	0.405	0.405	0.405	0.405	0.408	1%
2	1	2	1	0.280	0.280	0.280	0.280	0.280	0.280	0.280	0.285	2%
3	1	3	0.5	0.222	0.222	0.222	0.22	0.222	0.222	0.222	0.229	3%
4	2	1	1.25	0.580	0.580	0.580	0.580	0.580	0.580	0.580	0.580	0%
5	2	2	1.5	0.418	0.418	0.418	0.418	0.418	0.418	0.418	0.422	1%
6	2	3	2	0.330	0.330	0.330	0.330	0.330	0.330	0.330	0.334	1%
7	5	1	1	0.988	0.988	0.988	0.988	0.988	0.988	0.988	0.986	0%
8	5	2	1	0.754	0.754	0.754	0.754	0.754	0.754	0.754	0.759	1%
9	5	3	0.5	0.633	0.633	0.633	0.633	0.633	0.633	0.633	0.647	2%
10	10	1	1.25	1.328	1.328	1.328	1.328	1.328	1.328	1.328	1.318	1%
11	10	2	1.5	1.048	1.048	1.048	1.048	1.048	1.048	1.048	1.048	0%
12	10	3	2	0.856	0.856	0.856	0.856	0.856	0.856	0.856	0.858	0%
13	15	2	1	1.408	1.408	1.408	1.408	1.408	1.408	1.408	1.409	0%
14	15	2	1.5	1.300	1.300	1.300	1.300	1.300	1.300	1.300	1.297	0%
15	20	1	1	1.973	1.973	1.973	1.973	1.973	1.973	1.973	1.955	1%
16	20	2	1	1.645	1.645	1.645	1.645	1.645	1.645	1.645	1.644	0%
17	20	3	0.5	1.514	1.514	1.514	1.514	1.514	1.514	1.514	1.532	1%
18	25	2	2	1.572	1.572	1.572	1.572	1.572	1.572	1.572	1.561	1%
19	25	2	1.5	1.690	1.690	1.690	1.690	1.690	1.690	1.690	1.682	0%
20	30	2	1	2.038	2.038	2.038	2.038	2.038	2.038	2.038	2.033	0%
21	30	3	1.5	1.645	1.645	1.645	1.645	1.645	1.645	1.645	1.644	0%
22	40	2	1	2.364	2.364	2.364	2.364	2.364	2.364	2.364	2.354	0%
23	45	3	1.5	2.038	2.038	2.038	2.038	2.038	2.038	2.038	2.033	0%
24	50	5	1.25	1.845	1.845	1.845	1.845	1.845	1.845	1.845	1.855	1%
25	50	2	1.5	2.380	2.380	2.380	2.380	2.380	2.380	2.380	2.361	1%

26	50	3	2	2.011	2.011	2.011	2.011	2.011	2.011	2.011	2.00	1%
27	50	4	1.25	2.024	2.024	2.024	2.024	2.024	2.024	2.024	2.028	0%
28	60	3	1.5	2.364	2.364	2.364	2.364	2.364	2.364	2.364	2.353	0%
29	60	5	2	1.895	1.895	1.895	1.894	1.895	1.895	1.895	1.895	0%
30	65	3	1	2.695	2.695	2.695	2.695	2.695	2.695	2.695	2.691	0%
31	65	5	1.5	2.083	2.083	2.083	2.083	2.083	2.083	2.083	2.087	0%
32	70	5	1	2.309	2.309	2.309	2.309	2.309	2.309	2.309	2.321	1%
33	80	4	1	2.727	2.727	2.727	2.726	2.727	2.727	2.727	2.73	0%
34	100	2	1	3.719	3.719	3.719	3.719	3.719	3.719	3.719	3.688	1%
35	100	10	0.5	2.092	2.092	2.092	2.092	2.092	2.091	2.092	2.137	2%

***Table 11**: Validation test for critical depth in circular sections*

No	**q (m³/s)**	**d (m)**	**y_c (m)**						**Max. relative error (%)**
			Mohammadi (2016)	**Wong & Zhou (2004)**	**KC et al, (2010)**	**Ponce-Segovia et al., (2025)**	**Trial & error**	**Developed Model**	
1	1	1	0.573	0.573	0.573	-	0.573	0.572	0%
2	1	2	0.467	0.467	0.466	-	0.467	0.466	0%
3	1	3	0.417	0.417	0.417	-	0.417	0.417	0%
4	2	1	0.812	0.812	-	-	0.812	0.812	0%
5	2	2	0.666	0.666	0.666	-	0.666	0.666	0%
6	2	3	0.593	0.593	0.594	-	0.593	0.593	0%
7	5	1	0.991	0.991	-	-	0.991	0.993	0%
8	5	2	1.074	1.074	1.074	-	1.074	1.073	0%
9	5	3	0.95	0.95	0.95	-	0.95	0.95	0%
10	10	1	0.999	0.999	-	-	0.999	0.999	0%
11	10	2	1.533	1.533	1.533	-	1.533	1.533	0%
12	10	3	1.363	1.363	1.363	-	1.363	1.361	0%
13	20	1	0.1	0.1	-	-	0.1	0.1	0%
14	20	2	1.93	1.93	-	-	1.93	1.934	0%
15	20	3	1.957	1.957	1.957	-	1.957	1.955	0%
16	50	5	2.703	2.703	-	-	2.703	2.699	0%
17	50	2	1.998	1.998	-	-	1.998	1.999	0%
18	50	3	2.85	2.85	-	-	2.85	2.855	0%
19	50	4	2.885	2.885	-	-	2.885	2.884	0%
20	60	3	2.924	2.924	-	-	2.924	2.932	0%
21	60	5	2.973	2.973	-	-	2.973	2.969	0%
22	70	5	3.221	3.221	-	-	3.221	3.218	0%
23	80	4	3.554	3.554	-	-	3.554	3.557	0%

24	100	2	1.915	1.915	-	-	1.915	-	-
25	100	10	3.145	3.145	-	-	3.145	3.142	0%

Table 12*: Validation test for critical depth in rectangular sections*

No.	**q (m^3/s)**	**b (m)**	**y_c (m)**						**Max. relative error (%)**
			Mohammadi (2016)	**LetsConstruct (2012)**	**KC et al, (2010)**	**Ponce-Segovia et al., (2025)**	**Trial & error**	**Developed Model**	
1	1	1	0.467	0.467	0.467	0.467	0.467	0.467	0%
2	1	2	0.294	0.294	0.294	0.294	0.294	0.294	0%
3	1	3	0.225	0.225	0.225	0.225	0.225	0.225	0%
4	2	1	0.742	0.742	0.742	0.742	0.742	0.742	0%
5	2	2	0.467	0.467	0.467	0.467	0.467	0.467	0%
6	2	3	0.356	0.356	0.356	0.356	0.356	0.357	0%
7	5	1	1.366	1.366	1.366	1.366	1.366	1.366	0%
8	5	2	0.86	0.86	0.86	0.86	0.86	0.861	0%
9	5	3	0.657	0.657	0.657	0.657	0.657	0.657	0%
10	10	1	2.168	2.168	2.168	2.168	2.168	2.168	0%
11	10	2	1.366	1.366	1.366	1.366	1.366	1.366	0%
12	10	3	1.042	1.042	1.042	1.042	1.042	1.042	0%
13	20	1	3.442	3.442	3.442	3.442	3.442	3.44	0%
14	20	2	2.168	2.168	2.168	2.168	2.168	2.168	0%
15	20	3	1.655	1.655	1.655	1.655	1.655	1.654	0%
16	50	5	2.168	2.168	2.168	2.168	2.168	2.168	0%
17	50	2	3.994	3.994	3.994	3.994	3.994	3.991	0%
18	50	3	3.048	3.048	3.048	3.048	3.048	3.047	0%
19	50	4	2.516	2.516	2.516	2.516	2.516	2.515	0%
20	60	3	3.442	3.442	3.442	3.442	3.442	3.44	0%
21	60	5	2.448	2.448	2.448	2.448	2.448	2.448	0%
22	70	5	2.713	2.713	2.713	2.713	2.713	2.712	0%
23	80	4	3.442	3.442	3.442	3.442	3.442	3.44	0%
24	100	2	6.34	6.34	6.34	6.34	6.34	6.335	0%
25	100	10	2.168	2.168	2.168	2.168	2.168	2.167	0%

Table 13: Validation test for critical depth in triangular sections

No.	q (m^3/s)	z	y_c (m) Mohammadi (2016)	LetsConstruct (2012)	Wong & Zhou, (2004)	KC et al, (2010)	Ponce-Segovia et al., (2025)	Trial & error	Developed Model	Max. relative error (%)
1	1	1	0.728	0.728	0.728	0.728	0.728	0.728	0.727	0%
2	1	0.5	0.960	0.960	0.960	0.960	0.960	0.960	0.960	0%
3	2	1.25	0.878	0.878	0.878	0.878	0.878	0.878	0.878	0%
4	2	1.5	0.816	0.816	0.816	0.816	0.816	0.816	0.816	0%
5	2	2	0.728	0.728	0.728	0.728	0.728	0.728	0.728	0%
6	5	1	1.385	1.385	1.385	1.385	1.385	1.385	1.385	0%
7	5	0.5	1.828	1.828	1.828	1.828	1.828	1.828	1.827	0%
8	10	1.25	1.672	1.672	1.672	1.672	1.672	1.672	1.671	0%
9	10	1.5	1.554	1.554	1.554	1.554	1.554	1.554	1.554	0%
10	20	1	2.411	2.411	2.411	2.411	2.411	2.411	2.411	0%
11	20	0.5	3.182	3.182	3.182	3.182	3.182	3.182	3.180	0%
12	50	1.25	3.182	3.182	3.182	3.182	3.182	3.182	3.181	0%
13	50	1.5	2.958	2.958	2.958	2.958	2.958	2.958	2.957	0%
14	50	2	2.637	2.637	2.637	2.637	2.637	2.637	2.636	0%
15	60	1.5	3.180	3.180	3.180	3.180	3.180	3.180	3.180	0%
16	60	2	2.836	2.836	2.836	2.836	2.836	2.836	2.835	0%
17	70	1	3.980	3.980	3.980	3.980	3.980	3.980	3.980	0%
18	80	1	4.199	4.199	4.199	4.199	4.199	4.199	4.196	0%
19	100	1	4.590	4.590	4.590	4.591	4.590	4.590	4.588	0%
20	100	0.5	6.057	6.057	6.057	6.057	6.057	6.057	6.053	0%